

Kinetic and Thermodynamic Acidities of Pentacarbonyl(cyclobutenylidene)chromium Complexes. Effect of Antiaromaticity in the Conjugate Anion. An Experimental and Computational Study[†]

Claude F. Bernasconi,^{*,‡} Viola Ruddat,[‡] Philip J. Wenzel,[‡] and Helmut Fischer[§]

Department of Chemistry and Biochemistry of the University of California, Santa Cruz, California 95064, and the Department of Chemistry of the University of Konstanz, D-78434 Konstanz, Germany

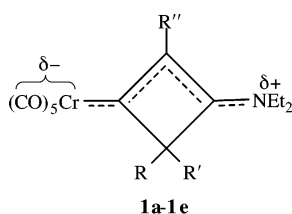
bernasconi@chemistry.ucsc.edu

Received April 5, 2004

The deprotonation of pentacarbonyl[(3-diethylamino-2,4-dimethyl)cyclobut-2-ene-1-ylidene]chromium (**1d**) and pentacarbonyl[(3-diethylamino-4-methyl-2-phenyl)cyclobut-2-ene-1-ylidene]chromium (**1e**) leads to antiaromatic conjugate anions by virtue of their being cyclobutadiene derivatives. Rate constants for the deprotonation of **1d** and **1e** by **P2-Et** and pK_a values were determined in acetonitrile. Gas-phase B3LYP calculations of **1d**, **1e**, and their respective conjugate anions, using a generalized basis set, were also performed. Furthermore, for purposes of comparison with carbene complexes of similar structures, but having conjugate anions that are not antiaromatic, corresponding calculations were performed on pentacarbonyl[3-diethylamino-2,5-dimethyl]cyclopent-2-ene-1-ylidene]chromium (**5**), [dimethylamino(methyl)carbene]pentacarbonylchromium (**3a**), and [dimethylamino(*iso*-propyl)carbene]pentacarbonylchromium (**3b**) and their respective conjugate anions, and solution-phase pK_a and kinetic measurements were carried out for **3a** and **3b**. Major points of interest include the effect of antiaromaticity on the kinetic and thermodynamic acidities of **1d** and **1e**, the large effect of the phenyl group on the gas-phase acidity of **1e**, the strong attenuation of the acidities and the effect of the phenyl group in acetonitrile, and the position of the C=C double bonds in the cyclobutadiene ring of the conjugate anion of **1e**.

Introduction

The synthesis and detailed characterization of the pentacarbonyl(cyclobutenylidene)chromium complexes



- a: R = R' = Ph, R'' = Me
- b: R, R' = (CH₂)₅, R'' = Me
- c: R = R' = Me, R'' = Me
- d: R = Me, R' = H, R'' = Me,
- e: R = Me, R' = H, R'' = Ph

1a-e has recently been reported.¹ A primary interest in

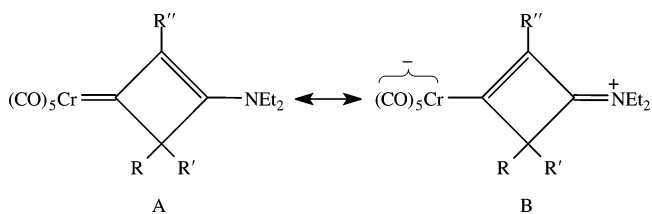
[†] Physical Organic Chemistry of Transition Metal Carbene Complexes. 30. Part 29: Bernasconi, C. F.; Bhattacharya, S. *Organometallics* **2004**, *23*, 1722.

[‡] University of California.

[§] University of Konstanz.

(1) Fischer, H.; Podschadly, O.; Roth, G.; Herminghaus, S.; Klewitz, S.; Heck, J.; Houbrechts, S.; Meyer, T. *J. Organomet. Chem.* **1997**, *541*, 321.

these Fischer-type carbene complexes² derives from their nonlinear optical properties which are related to the push-pull electronic structure symbolized by the strong contribution of the resonance form B.¹



Two of these complexes, **1d** and **1e**, have an acidic proton which can be removed in the presence of a strong

(2) Dötz, K. H.; Fischer, H.; Hofmann, P.; Kreissl, F. R.; Schubert, U.; Weiss, K. *Transition Metal Complexes*; Verlag Chemie: Deerfield Beach, FL, 1983.

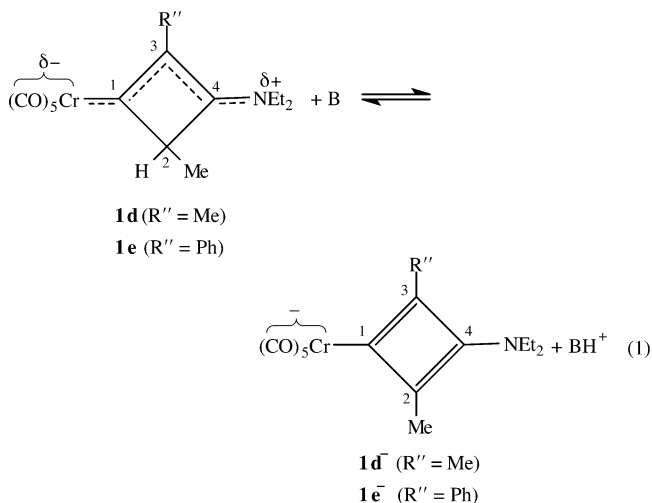
(3) (a) Bernasconi, C. F.; *Chem. Soc. Rev.* **1997**, *26*, 299. (b) Bernasconi, C. F. *Adv. Phys. Org. Chem.* **2002**, *37*, 137.

(4) As shown below, ab initio calculations on **1e**⁻ indicate double bonds C1-C3 and C2-C4 rather than C1-C2 and C3-C4; for **1d**⁻ which is symmetrical both representations are equivalent.

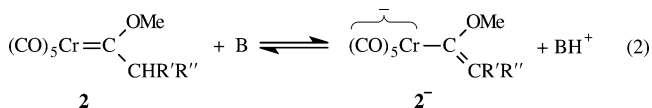
(5) The intrinsic barrier, ΔG_0^\ddagger (intrinsic rate constant, k_0), of a reaction with a forward rate constant k_1 and a reverse rate constant k_{-1} is defined as $\Delta G_0^\ddagger = \Delta G_1^\ddagger = \Delta G_{-1}^\ddagger$ ($k_0 = k_1 = k_{-1}$) when $\Delta G_0 = 0$ ($K_1 = 1$).

(6) Bernasconi, C. F.; Leyes, A. E.; Ragains, M. L.; Shi, Y.; Wang, H.; Wulff, W. D. *J. Am. Chem. Soc.* **1998**, *120*, 8632.

base, eq 1. What is unique about these systems is that,



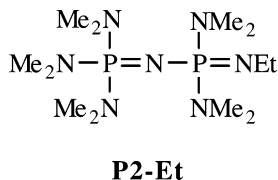
unlike other Fischer carbene complexes that contain acidic protons such as **2** and similar compounds,³ deprotonation of **1d** and **1e** generates conjugate bases (**1d**⁻, **1e**⁻) that are antiaromatic by virtue of their cyclobutadiene ring.⁴ Hence, one would expect that the thermodynamic acidity of **1d** and **1e** should be depressed relative to that of other carbene complexes.



What is less predictable is the effect of the antiaromaticity on the intrinsic barrier or intrinsic rate constant⁵ of the reaction, i.e., the kinetic acidity. In this paper, we present experimental data on the kinetic and thermodynamic acidities of **1d** and **1e** in acetonitrile and results of gas phase ab initio calculations of the structures and thermodynamic acidities of these carbene complexes. We show that in the gas phase the effect of antiaromaticity on the thermodynamic acidities is large but strongly attenuated in acetonitrile. We also conclude that the intrinsic barrier to proton transfer is relatively low, which suggests that antiaromaticity may have a barrier-lowering effect.

Results

Spectrophotometric pK_a Determination. **1d** and **1e** are much weaker acids than typical Fischer carbene complexes such as **3**⁶ but they can be deprotonated by 1-ethyl-2,2,4,4,4-pentakis(dimethylamino)-2*R*,⁵4*R*⁵-catenadi(phosphazene), **P2-Et**, whose pK_a in acetonitrile is 32.8.⁷



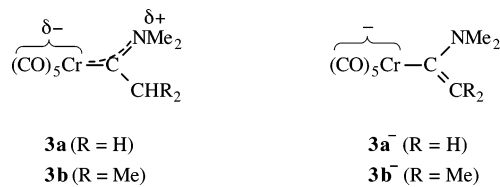
The deprotonation of **1d** and **1e** is associated with a decrease in absorption and a hypsochromic shift. This al-

TABLE 1. pK_a Values and Rate Constants for the Deprotonation of **1d**, **1e**, **3a**, and **3b** by **P2-Et** in Acetonitrile 25 °C

carbene complex	pK_a	$pK_a^{\text{corr } a}$	$k_1 (\text{M}^{-1} \text{s}^{-1})$	$k_1^{\text{corr}} (\text{M}^{-1} \text{s}^{-1})^a$
1d	34.6 ± 0.2	34.3 ± 0.2	10.0 ± 0.5	10.0 ± 0.5
1e	33.9 ± 0.2	33.9 ± 0.2	7.24 ± 0.25	7.24 ± 0.25
3a	31.9 ± 0.4	32.4 ± 0.4	210 ± 20	70 ± 7
3b	32.4 ± 0.3	32.4 ± 0.3	0.183 ± 0.013	0.183 ± 0.013
2 ($\text{R}' = \text{R}'' = \text{H}$) ^b	22.2 ± 0.2	22.7 ± 0.2		

^a Statistically corrected for the number of equivalent protons of the carbene complex and equivalent basic sites on the anion.
^b Reference 6.

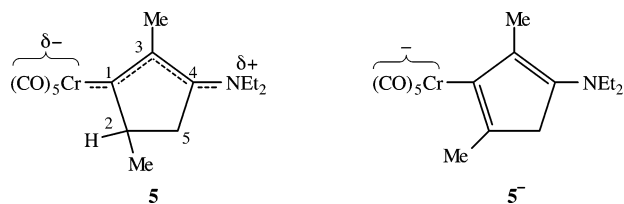
lowed a spectrophotometric determination of their pK_a values as described in the Experimental Section. In contrast to the situation with **2** and similar carbene complexes, the deprotonation of **1d** and **1e** is relatively slow. Because the respective anions are not very stable, this means that there is some decomposition of the anions before the deprotonation is complete, necessitating extrapolation of the absorbance values to “zero time.” For comparison purposes, the acidity of **3b** was also determined, using the same methodology; the pK_a of **3a** has been determined before.⁸ The various pK_a values are reported in Table 1.



Rates of Deprotonation. Kinetic experiments were run under pseudo-first-order conditions with a large excess of **P2-Et**. The reaction was shown to be strictly first order in **P2-Et** over a concentration range from 4×10^{-4} to 3×10^{-3} M. Second-order rate constants, k_1 , for the deprotonation reaction were obtained from the slopes of k_{obsd} versus [**P2-Et**]; they are reported in Table 1.

Calculations. DFT calculations using the B3LYP density functional were performed on **1d**, **1e**, **3a**, and **3b** and their respective anions **1d**⁻, **1e**⁻, **3a**⁻, and **3b**⁻.

In our experimental study we have used **3a** and **3b** as models for carbene complexes with a strong π -donor group (Me_2N) but whose respective conjugate bases are not antiaromatic and hence may be compared with **1d** and **1e** to assess the effect of antiaromaticity on acidity and rate constants. This choice of models is not optimal but was dictated by the availability/accessibility of known Fischer carbenes. A better model is the carbene complex **5** which is both cyclic and includes the same push-pull system as **1d** and **1e**. Even though **5** is not a known compound, calculations on it and its conjugate base **5**⁻ were performed.



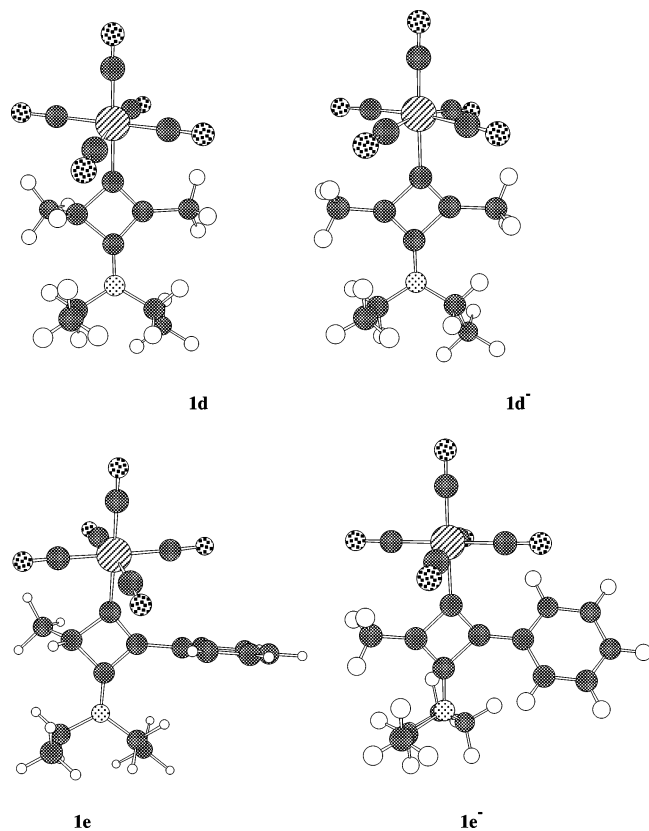


FIGURE 1. Structures of **1d**, **1d⁻**, **1e**, and **1e⁻**.

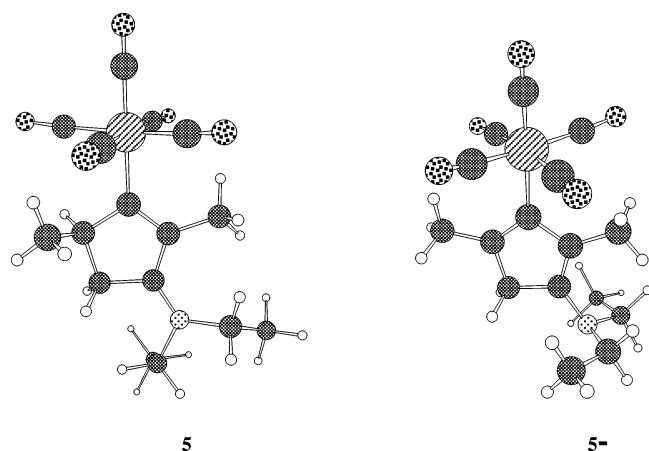


FIGURE 2. Structures of **5** and **5⁻**.

To keep the calculations at a manageable level for **1d**, **1d⁻**, **1e**, **1e⁻**, **5**, and **5⁻**, a generalized basis set was used as described in the Experimental Section. For consistency, the same generalized basis set was also used for **3a**, **3a⁻**, **3b**, and **3b⁻**.

Figure 1 shows the optimized (at B3LYP level) structures of **1d**, **1d⁻**, **1e**, and **1e⁻**, respectively, while the structures of **5** and **5⁻** are displayed in Figure 2 and those of **3a**, **3a⁻**, **3b** and **3b⁻** in Figure 3. Tables 2–4 summarize relevant bond lengths and dihedral angles. For the anion of **1e** two structures were calculated: **1e⁻** is

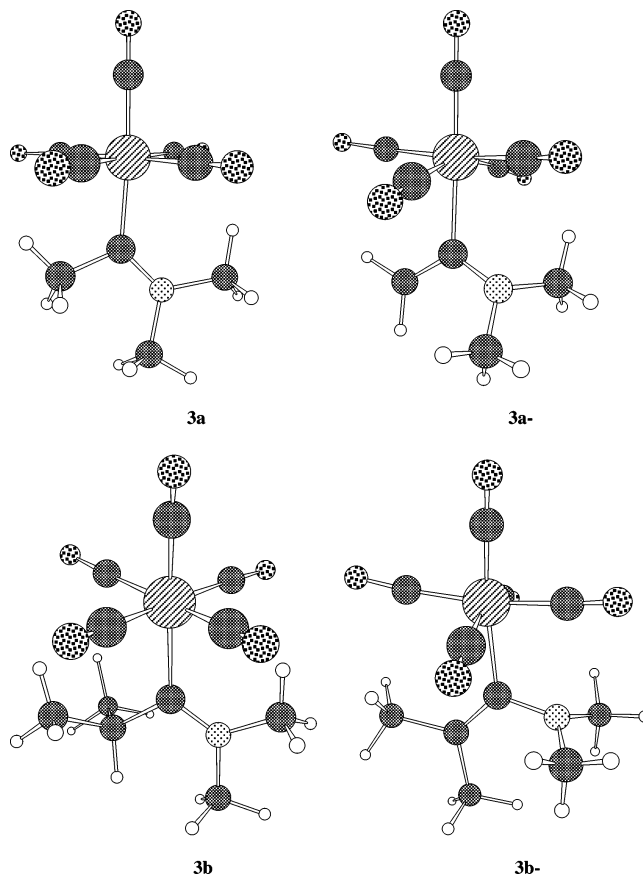
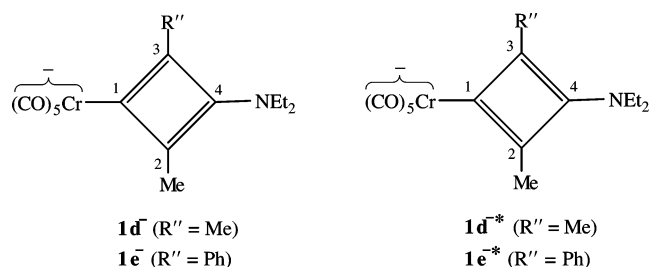


FIGURE 3. Structures of **3a**, **3a⁻**, **3b**, and **3b⁻**.

the optimized structure with the double bonds C1–C3 and C2–C4, and **1e^{-*}**, a higher energy structure, with double bonds constrained to C1–C2 and C3–C4. Note that for the anion of **1d** the two structures, **1d⁻** and **1d^{-*}**, are identical. Table 2 also includes experimental bond lengths for the model system **1b**.



NPA group charges (at the B3LYP level) are summarized in Figures 4–6 while Table 5 reports the gas-phase acidities. More complete computational results are summarized in Tables S1–S3 (geometries) and Table S4 (energies) of the Supporting Information.⁹

Discussion

Computational Results. The computed bond lengths for **1d** and **1e** are quite similar to each other as well as to those calculated and determined by X-ray crystal-

(7) Dega-Szafran, Z.; Schroeder, G.; Szafran, M. *J. Phys. Org. Chem.* **1999**, *12*, 39.

(8) Bernasconi, C. F.; Ragains, M. L. To be published.

(9) See the Supporting Information paragraph.

TABLE 2. Bond Lengths and Dihedral Angles (B3LYP) for 1d, 1d⁻, 1e, 1e⁻, 1e^{-*}, and 1b^a

bond or dihedral angle	1d	1d ⁻	Δ^b	1e	1e ⁻	Δ^c	1e ^{-*}	1b (exp) ^d
C=O trans	1.173	1.183	0.010	1.173	1.183	0.010	1.184	n.r.
C=O cis	1.175	1.178	0.003	1.175	1.180	0.005	1.180	n.r.
Cr–CO trans	1.886	1.836	-0.050	1.888	1.853	-0.035	1.850	1.815
Cr–CO cis	1.882	1.867	-0.015	1.884	1.867	-0.017	1.875	1.902
Cr=C1	2.003	2.091	0.088	1.994	2.076	0.082	2.085	2.100
C1–C3	1.406	1.352	-0.054	1.408	1.375	-0.033	1.587	1.390
C1–C2	1.557	1.588	0.031	1.558	1.566	0.008	1.365	1.572
C3–C4	1.412	1.563	0.151	1.412	1.563	0.151	1.381	1.428
C2–C4	1.517	1.354	-0.163	1.520	1.352	-0.168	1.523	1.542
C4–N	1.329	1.389	0.060	1.326	1.389	0.063	1.364	1.315
C3–C5				1.473	1.435	-0.038	1.429	1.512
CO cis 1–Cr–C1–C2	-42.4	-39.0		-80.0	-34.8		-39.41	-97.7
CO cis 2–Cr–C1–C2	48.4	50.8		10.5	55.3		51.82	10.3
C1–C3–C5–C6				73.5	142.7		142.1	
C1–C2–C3–C4	-4.5	-0.7		10.1	-0.4		4.12	6.7

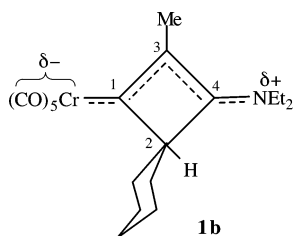
^a Bond lengths in angstroms, angles in degrees. ^b 1d⁻ – 1d. ^c 1e⁻ – 1e. ^d From X-crystal structure data, ref 1.

TABLE 3. Bond Lengths and Dihedral Angles (B3LYP) for 5 and 5⁻^a

bond or dihedral angle	5	5 ⁻	Δ^b
C=O trans	1.175	1.186	0.011
C=O cis	1.176	1.181	0.005
Cr–CO trans	1.882	1.852	-0.030
Cr–CO cis	1.889	1.878	-0.011
	1.802	1.871	-0.011
	1.910	1.875	-0.035
	1.889	1.897	-0.008
Cr=C1	2.095	2.201	0.106
C1–C3	1.409	1.504	0.095
C1–C2	1.527	1.367	-0.160
C3–C4	1.420	1.361	-0.059
C4–C5	1.504	1.501	-0.003
C2–C5	1.541	1.511	-0.030
C4–N	1.341	1.433	0.092
CO cis 1–Cr–C1–C3	-28.9	-53.2	
CO cis 2–Cr–C1–C3	63.2	38.5	
C1–C3–C4–C5	-4.5	-1.2	
C2–C1–C3–C4	5.6	0.8	

^a Bond lengths in angstroms, angles in degrees. ^b 5⁻ – 5.

lography for 1b.¹ In particular, the C1–C3 and C3–C4



bonds are much shorter than the C1–C2 and C2–C4 bonds due to their partial double-bond character. As pointed out before,¹ the C1–C3 bond is even somewhat shorter than the C3–C4 bond, implying that resonance structure B is dominant. The respective bond lengths for 5 are also quite similar to those for 1d although the Cr–C1, C1–C3, C3–C4, and C4–N bonds in 5 are all slightly longer than the corresponding bonds in 1d while the C1–C2 bond is somewhat shorter. A detailed interpretation of these differences is difficult to come by except to say that they must be related to the change from a four-membered to a five-membered ring.

The changes in the bond lengths upon conversion of the cyclobutenylidene complexes into their respective anions are also quite similar for 1d and 1e. The lengthening of the C=O and shortening of the Cr–CO bond lengths are the result of charge delocalization into the

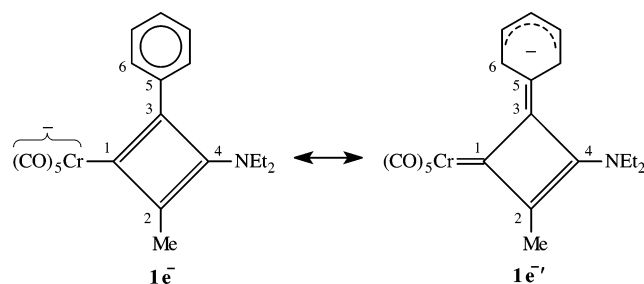
CO ligands, while the lengthening of the Cr=C1 and the C4–N bonds reflects the loss of their partial double bond character. The bond changes within the four-membered ring are particularly noteworthy because the shortening of the C1–C3 and C2–C4 implies that the position of the double bonds in the anion of 1e is that in 1e⁻ rather than in 1e^{-*}; as discussed below, 1e⁻ is 0.78 kcal/mol lower in energy than 1e^{-*}.

For the conversion of 5 to 5⁻, similar changes in the C=O, Cr–CO, Cr–C1, and C4–N bonds are observed as for the conversion of 1d to 1d⁻ and 1e to 1e⁻. In contrast, the C1–C3 bond of 5⁻ is lengthened while the C1–C2 and C3–C4 bonds are shortened, reflecting the facts that in 5⁻ it is the C1–C2 and C3–C4 bonds rather than the C1–C3 and C2–C4 bonds that adopt double bond character.

For 3a and 3b, the pattern in the bond changes upon conversion to the respective anions are as one would expect: slight lengthening of the C=O bonds, shortening of the Cr–CO bonds, substantial lengthening of the Cr–C1 and C1–N bonds and substantial shortening of the C1–C2 bonds.

Turning to the gas-phase acidities reported in Table 5, we note that 1d and 1e are substantially less acidic than 5, 3a and 3b. The largest difference is between 1d and 5 with 1d being 35 kcal/mol less acidic than 5. The low acidity of 1d and 1e can be attributed to the destabilization of 1d⁻ and 1e⁻ due to their antiaromatic character.¹⁰

The higher acidity of 1e compared to that of 1d ($\Delta\Delta H^\circ = 7.8$ kcal/mol) suggests that the phenyl group in 1e⁻ acts as a π -acceptor (1e⁻ \leftrightarrow 1e^{-'}). This interpretation is



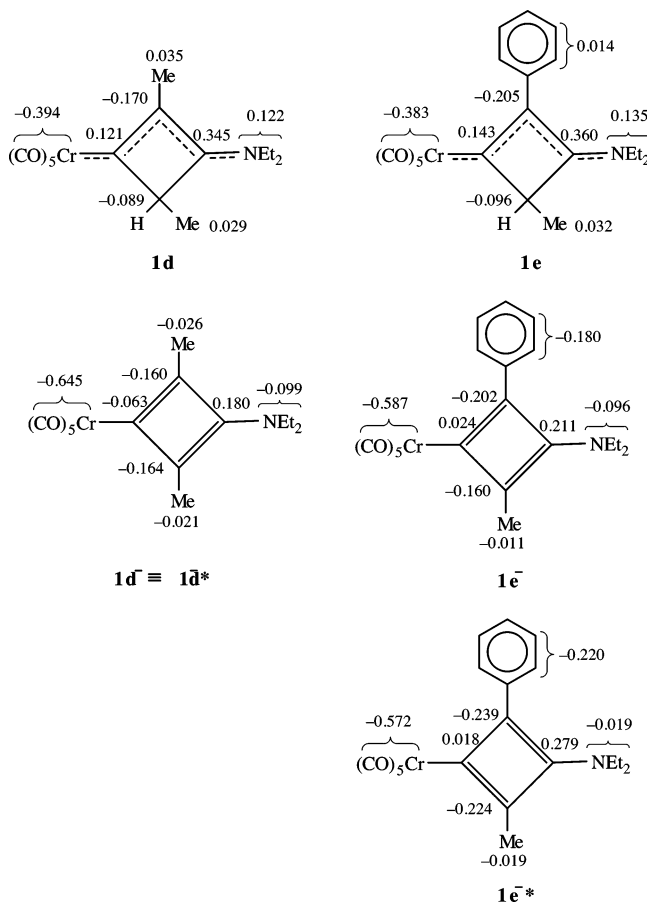
supported by three observations. (1) The C1–C3 bond

(10) According to a recent MP4(SDQ)/6-31G(d,p) calculation the absolute antiaromaticity of cyclobutadiene is 40.28 kcal/mol.¹¹

TABLE 4. Bond Lengths and Dihedral Angles (B3LYP) for 3a, 3a⁻, 3b, and 3b⁻

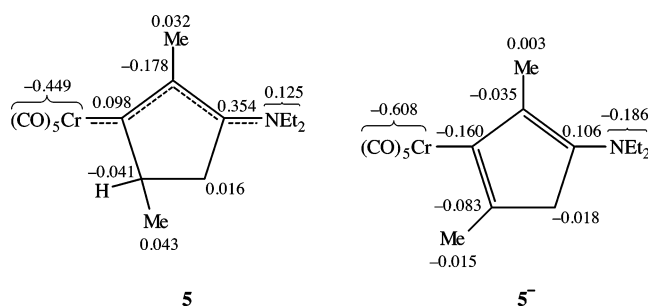
bond or dihedral angle	3a	3a ⁻	Δ^b	3b	3b ⁻	Δ^c	3a (exp)
C=O trans	1.173	1.183	0.010	1.173	1.816	0.013	1.160
C=O cis	1.174	1.185	0.011	1.175	1.186	0.011	1.130
Cr–CO trans	1.880	1.858	-0.022	1.876	1.844	-0.032	1.850
Cr–CO cis	1.883	1.843	-0.040	1.885	1.883	-0.002	1.860
Cr–C1	2.084	2.189	0.105	2.127	2.195	0.068	2.160
C1–C2 ^e	1.520	1.356	-0.164	1.330	1.351	-0.184	1.500
C1–N	1.327	1.429	0.102	1.535	1.450	0.120	1.310
CO cis 1- Cr–C1–C2	45.41	-9.03		-21.88	1.00		
CO cis 2- Cr–C1–C2	46.54	80.94		68.61	88.4		

^a Bond lengths in Å, angles in degrees. ^b 3a⁻ – 3a. ^c 3b⁻ – 3b.

**FIGURE 4.** NPA group charges (at B3LYP level) for **1d**, **1d⁻**, **1e**, **1e⁻**, and **1e^{*}**.

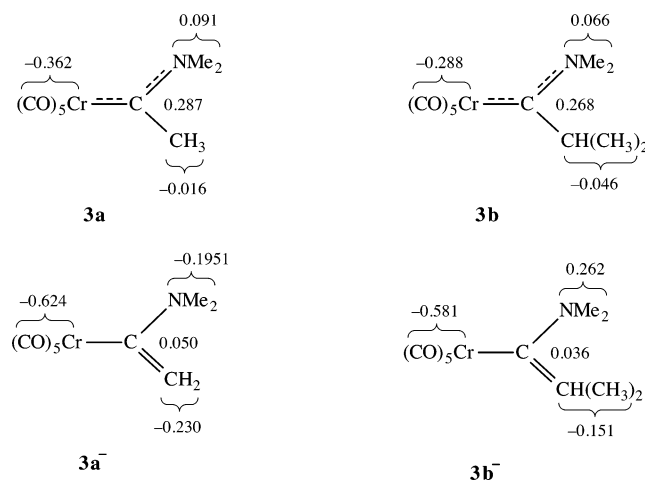
contraction upon deprotonation of **1e** (-0.033 Å) is smaller than that for the deprotonation of **1d** (-0.054 Å). (2) The deprotonation of **1e** induces the phenyl group to change its orientation from nearly perpendicular (dihedral angle C1–C3–C5–C6 of 73.5°) to more coplanar (dihedral angle C1–C3–C5–C6 of 142.7°). (3) As is shown in Figure 4, there is a significant negative charge on the phenyl group of **1e⁻** (-0.180) while the negative charge on the $(\text{CO})_5\text{Cr}$ moiety (-0.587) is significantly lower than that on **1d⁻** (-0.645).

The fact that in the conjugate base of **1e** the preferred position of the double bonds in the cyclobutadiene ring is that of structure **1e⁻** rather than **1e^{*}** suggests a mechanism of the deprotonation reaction. Two mecha-

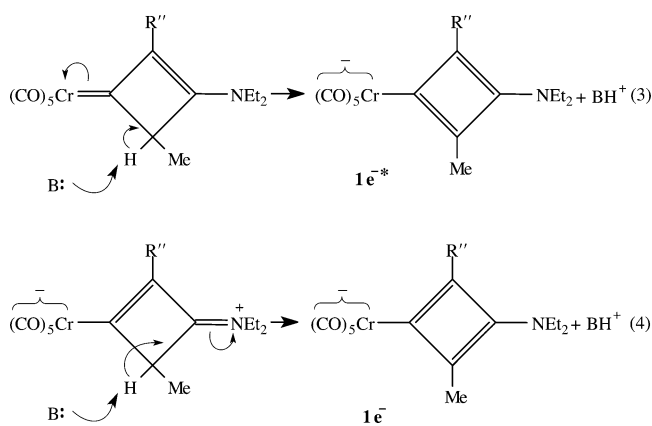
**FIGURE 5.** NPA group charges (at B3LYP level) for **5** and **5⁻**.**TABLE 5. Gas Phase Acidities at 25°C**

	ΔE (kcal/mol)	ΔZPE (kcal/mol)	ΔHP (kcal/mol)	$\Delta\Delta HP$ (kcal/mol)
1d → 1d⁻ + H ⁺	378.6	-9.0	369.6	
1e → 1e⁻ + H ⁺	370.8	-9.0	361.8	7.8 ^a
3a → 3a⁻ + H ⁺	348.6	-7.7	340.9	
3b → 3b⁻ + H ⁺	345.9	-9.9	336.0	4.9 ^b
5 → 5⁻ + H ⁺	344.5	-9.7	334.8	

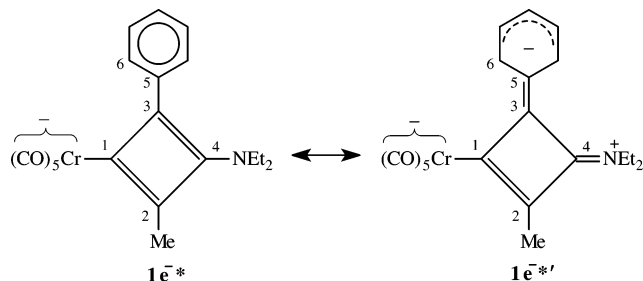
^a $\Delta H^\circ(\mathbf{1d}) - \Delta H^\circ(\mathbf{1e})$. ^b $\Delta H^\circ(\mathbf{3a}) - \Delta H^\circ(\mathbf{3b})$.

**FIGURE 6.** NPA group charges (at B3LYP level) for **3a**, **3a⁻**, **3b**, and **3b⁻**.

nistic pathways may be visualized, eqs 3 and 4, depending on which resonance structure of **1d** or **1e** is chosen to represent the carbene complex. Our results support the mechanism of eq 4.¹²

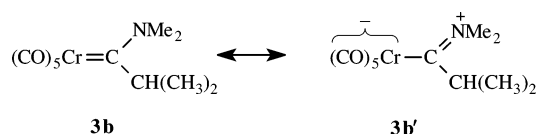


Regarding possible reasons why $1e^-$ is more stable than $1e^{-*}$, we note the following. As pointed out above, charge delocalization into the phenyl ring ($1e^-$) helps stabilize $1e^-$ but the NPA group charges indicate a similar delocalization of negative charge into the phenyl group of $1e^{-*}$ that may be understood in terms of the resonance structure $1e^{-*'}$. The fact that the C4–N bond



in $1e^{-*}$ (1.364 Å) is shorter than $1e^-$ (1.389 Å) is consistent with a contribution by $1e^{-*'}$. Hence, the main reason for the different stabilities is probably not electronic but steric, i.e., steric crowding between the phenyl group and the Et₂N group may be more severe than that between the phenyl group and the (CO)₅Cr moiety. Thus, elongating the C3–C4 rather than the C1–C3 bond would bring about greater relief of steric strain.

Regarding **3a** and **3b**, the structures of these carbene complexes are too different from that of **5** to allow a detailed explanation as to why their acidities are somewhat lower than that of **5**. However, a comparison between **3a** and **3b** is in order. The higher acidity of **3b** relative to that of **3a** ($\Delta\Delta H^\ddagger = 4.9$ kcal/mol) is probably the combined result of a destabilization of the zwitterionic structure **3b'** due to steric interference by the isopropyl group and an enhanced stabilization of the C=C double bond in **3b'** by the methyl groups.¹⁴ A reduced contribution of **3b'** to the resonance hybrid is consistent with the smaller negative charge on the (CO)₅Cr moiety and the smaller positive charge in the Me₂N group of **3b** relative to the same charges in **3a**.



Results in Acetonitrile. In acetonitrile the acidity differences between the cyclobutenylidene complexes (**1d**, **1e**) and dimethylamino carbene complexes (**3a**, **3b**) are much smaller than in the gas phase; e.g., the measured¹⁵ pK_a of **1d** (34.6) is only 2.7 units higher than that of **3a**

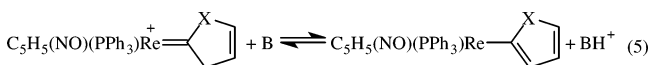
(31.9) (Table 1) which, in enthalpy terms, corresponds to a 3.5 kcal/mol difference.

The main difference between solution and gas phase must be the solvation of the charges in the partially zwitterionic carbene complexes and their respective anions. The solvation of **1d**⁻ and **3a**⁻ is probably quite similar. On the other hand, solvational stabilization of **3a** is expected to be stronger than that of **1d** because the more extended π -system in **1d** provides more internal stabilization. This results in a reduction of the acidity of **3a** relative to that of **1d**.

The acidity difference between **1d** and **1e**, and that between **3a** and **3d**, are also strongly attenuated in acetonitrile. For **1d** versus **1e** this attenuation may be related to a stronger solvation of **1d**⁻ because in **1d**⁻ the negative charge is more concentrated on the (CO)₅Cr moiety than in **1e**⁻ (Figure 4), and hence, the strong solvation partially offsets the greater internal stabilization of **1e**⁻ by the phenyl group that manifests itself in the gas phase. With **3a** versus **3b**, the steric destabilization of **3b'** that occurs in the gas phase may be attenuated because solvation can support larger charges on the (CO)₅Cr and Me₂N moieties, resulting in a lower acidity of **3b** and making the pK_a values of **3a** and **3b** about the same.

A question of major interest is whether the fact that the deprotonation of **1d** and **1e** leads to anions with an antiaromatic cyclobutadiene ring has a significant effect on the intrinsic barriers or intrinsic rate constants⁵ of these reactions, and whether a comparison between **1d** and **1e** on one hand and **3a** and **3b** on the other allows such a determination. If the development of antiaromaticity at the transition state has made less progress than proton transfer, there should be a decrease in the intrinsic barrier or an increase in the intrinsic rate constant; if the development of antiaromaticity has made more progress than proton transfer at the transition state, ΔG^\ddagger should increase and k_0 should decrease.¹⁶

It has recently been suggested that development of aromaticity is ahead of proton transfer in the deprotonation of cyclic rhenium carbene complexes such as **4H**⁺(X) where the conjugate bases **4(X)** contain the furan, thiophene and selenophene rings, respectively.¹⁸ This



conclusion was somewhat surprising because it is op-

(11) Suresh, C. H.; Koga, N. *J. Org. Chem.* **2002**, *67*, 1965.

(12) A reviewer suggested that eqs 3 and 4 may not be really different because they are related via resonance. It is our contention that they are different because $1e^-$ and $1e^{-*}$ are not resonance structures but different compounds, a well-known feature of cyclobutadienes.¹³

(13) Minkin, V. I.; Glukhovtsev, M. N.; Simkin, B. Y. *Aromaticity and Antiaromaticity*; Wiley & Sons: New York, 1994; pp 138–141.

(14) The stabilization of alkenes by methyl groups is a well-known phenomenon, see, e.g.: McMurry, J. *Organic Chemistry*; Brooks/Cole: Belmont, CA, 2003; p 183.

(15) When calculating and comparing enthalpies, the use of the experimental, i.e., statistically uncorrected pK_a values, is more appropriate.

(16) These predictions are based on the Principle of Nonperfect Synchronization (PNS).¹⁷ The PNS states that the intrinsic barrier of a reaction increases if the development of a product stabilization factor (e.g., resonance or solvation) lags behind bond changes but decreases if the development of the product stabilization factor runs ahead of bond changes. Conversely, if a product destabilizing (e.g., antiaromaticity) lags behind bond changes the intrinsic barrier decreases while the intrinsic barrier increases if the product destabilizing factor is ahead of bond change.

(17) (a) Bernasconi, C. F. *Acc. Chem. Res.* **1987**, *20*, 301. (b) Bernasconi, C. F. *Acc. Chem. Res.* **1992**, *25*, 9. (c) Bernasconi, C. F. *Adv. Phys. Org. Chem.* **1992**, *27*, 119.

(18) Bernasconi, C. F.; Ragains, M. L.; Bhattacharya, S. *J. Am. Chem. Soc.* **2003**, *125*, 12328.

posite to the situation with ordinary resonance/delocalization effects, i.e., the development of these latter effects always lags behind proton transfer at the transition state.^{17,19} Furthermore, ab initio calculations of gas-phase identity proton transfers in systems such as benzenium ion/benzene and cyclopentadiene/cyclopentadienyl anion also indicated that aromaticity is more than 50% developed at the transition state.²³ These results suggest that the constraints that prevent extensive development of “ordinary” resonance stabilization at the transition state^{17,21d,24} may not apply to the development of aromaticity.

Because of the interrelatedness of aromaticity and antiaromaticity it would seem plausible that the latter would follow the pattern observed with the former, i.e., antiaromaticity develops ahead of proton transfer, thereby raising the intrinsic barrier or lowering the intrinsic rate constant. On the other hand, if the development of antiaromaticity were to lag behind proton transfer, as is the case for ordinary resonance effects, this could lower the energy of the transition state and hence would be a more advantageous situation.

Our results do not allow a definite conclusion on this point because several factors other than antiaromaticity may affect the intrinsic rate constants of the reactions of **1d** and **1e** relative to those of the reactions of **3a** and **3b**. Nevertheless, the following discussion should provide some important insights. The k_1^{corr} value for the deprotonation of **1d** by **P2-Et** is 7-fold lower than for **3a** (Table 1) but this reduction can be accounted for by the higher pK_a^{corr} . Applying the simplest version of the Marcus²⁵ equation to the ratio of the rate constants, eq 6, yields

$$\log \frac{k_0(\mathbf{1d})}{k_0(\mathbf{3a})} = \frac{k_1^{\text{corr}}(\mathbf{1d})}{k_1^{\text{corr}}(\mathbf{3a})} + 0.5 \log \frac{k_a^{\text{corr}}(\mathbf{3a})}{k_a^{\text{corr}}(\mathbf{1d})} \quad (6)$$

$\log(k_0^{\text{corr}}(\mathbf{1d})/k_0^{\text{corr}}(\mathbf{3a})) = 0.105$, i.e., the intrinsic rate constants for the two reactions are virtually the same. An interpretation of this result requires an examination of the factors that distinguish **1d** and **1e** from **3a**, factors that may potentially affect the relative intrinsic rate constants for proton transfer. These factors include the overall structure of the respective carbene complexes, steric effects, the degree of push–pull resonance and the antiaromaticity of **1d⁻** and **1e⁻**.

1. Overall Structure. The structures of **1d** and **1e** are sufficiently different from that of **3a** that they may lead to different “baseline” intrinsic rate constants for **1d** and **1e** relative to **3a**. If this is the case we cannot predict which “baseline” intrinsic barrier may be the higher one.

2. Steric Effect. The transition state for the deprotonation of **1d** and **1e** is expected to be more crowded than that for the deprotonation of **3a** because the proton in **1d** and **1e** is on a tertiary carbon. This will reduce k_0 for **1d** and **1e** relative to that for **3a**. Due to the large size of the base (**P2-Et**), this reduction may be substantial as the large decrease in k_1^{corr} for the more crowded **3b** relative to **3a** suggests.

3. Push–Pull Resonance. The effect of this factor on k_0 is difficult to predict because two opposing influences are involved. One is the loss of the resonance stabilization of the carbene complex ($A \leftrightarrow B$) upon deprotonation which must follow the general rule that applies to resonance effects, i.e., its loss must be ahead of proton transfer at the transition state.^{17,19} The result is a reduction in k_0 . The other effect of the push–pull resonance of the carbene complex is an attenuation of the lag in resonance development of the anion. This comes about because the contribution of B (for **1d** and **1e**) or **3'** to the structure of the respective carbene complexes leads to a preorganization of the (CO)₅Cr moiety toward its electronic configuration in the anion. This should result in a stabilization of the transition state due to greater charge delocalization into the (CO)₅Cr moiety, leading to a lower intrinsic barrier or a larger k_0 . As discussed in more detail elsewhere,²⁶ there are precedents for either of these factors to be dominant. It appears that in systems with the strongest push–pull resonance, the second factor is dominant which leads to an increase in k_0 ,²⁷ while in systems where the push–pull resonance is weaker, the first factor dominates and k_0 is reduced.²⁸ To the extent that the push–pull effect is particularly strong in **1d** and **1e** one might expect k_0 for **1d** and **1e** to increase relative to that for **3a** but this conclusion is not firm.

4. Antiaromaticity. Based on our earlier discussion, k_0 for **1d** and **1e** should be enhanced relative to k_0 for **3a** if antiaromaticity lags behind proton transfer but should be reduced if antiaromaticity develops ahead of proton transfer. The fact that the experimental k_0 values for **1d** and **3a** are about the same despite the steric effect implies that one, two or all three factors discussed above, i.e., overall structure, push–pull resonance and antiaromaticity act to offset the steric effect by enhancing k_0 for **1d** and **1e**. Unless the “baseline” k_0 values for **1d** and **1e** are significantly higher than for **3a**, it is unlikely that the push–pull resonance effect alone is sufficient to offset the steric effect. This would suggest that the antiaromaticity factor contributes to the enhancement of k_0 , implying that antiaromaticity development lags behind proton transfer. However, further work on systems where factors other than antiaromaticity can be excluded will be needed to find a more definite answer.

Conclusions

(1) In the gas phase **1d** and **1e** are much less acidic than **5**, **3a**, or **3b**, presumably mainly because **1d⁻** and

(19) This is also true for gas-phase proton transfers.^{20–22}

(20) (a) Saunders, W. H., Jr. *J. Am. Chem. Soc.* **1994**, *116*, 5400. (b) Saunders, W. H., Jr.; Van Verth, J. E. *J. Org. Chem.* **1995**, *60*, 3452.

(21) (a) Bernasconi, C. F.; Wenzel, P. J. *J. Am. Chem. Soc.* **1994**, *116*, 5405. (b) Bernasconi, C. F.; Wenzel, P. J. *J. Am. Chem. Soc.* **1996**, *118*, 10494. (c) Bernasconi, C. F.; Wenzel, P. J.; Keeffe, J. R.; Gronert, S. *J. Am. Chem. Soc.* **1997**, *119*, 4008. (d) Bernasconi, C. F.; Wenzel, P. J. *J. Org. Chem.* **2001**, *66*, 968.

(22) Lee, I.; Kim, C. K.; Kim, C. K. *J. Phys. Org. Chem.* **1999**, *12*, 255.

(23) Bernasconi, C. F.; Ragains, M. L. To be published.

(24) Kresge, A. J. *Can. J. Chem.* **1974**, *52*, 1897.

(25) (a) Marcus, R. A. *Annu. Rev. Phys. Chem.* **1964**, *15*, 155. (b) Marcus, R. A. *J. Phys. Chem.* **1968**, *72*, 891.

(26) Bernasconi, C. F.; Ali, M. *J. Am. Chem. Soc.* **1999**, *121*, 3039.

(27) (a) Bernasconi, C. F.; Renfrow, R. A.; Tia, P. R. *J. Am. Chem. Soc.* **1986**, *108*, 4541. (b) Bernasconi, C. F.; Zitomer, J. L.; Schuck, D. F. *J. Org. Chem.* **1992**, *57*, 1132.

(28) (a) Bernasconi, C. F.; Panda, M. *J. Org. Chem.* **1987**, *52*, 3042. (b) Bernasconi, C. F.; Killion, R. B., Jr. *J. Org. Chem.* **1989**, *54*, 2878. (c) Bernasconi, C. F.; Flores, F. X.; Claus, J. J.; Dvořák, J. *J. Org. Chem.* **1994**, *59*, 4917.

$1e^-$ are antiaromatic. Solvation effects in acetonitrile strongly attenuate these acidity differences.

(2) Replacing the methyl group in **1d** with a phenyl group (**1e**) enhances the gas-phase acidity by 7.8 kcal/mol. This can be attributed to partial delocalization of the anionic charge into the phenyl group, consistent with computed bond lengths, dihedral angles, and NPA group charges.

(3) The anionic structure of $1e^-$ is 0.78 kcal/mol more stable than $1e^{*-}$. A possible reason is that a longer C3–C4 bond ($1e^-$) alleviates more steric strain than a longer C1–C3 bond ($1e^{*-}$).

(4) The measured rate constants for the deprotonation of **1d** by **P2-Et** suggest that the *intrinsic* rate constant is about the same as for the deprotonation of **3a** by the same base. However, in the absence of steric effects, the “true” k_0 value for **1d** would be significantly higher than for **3a**. A possible interpretation of this enhanced intrinsic rate constant is that the development of antiaromaticity lags behind proton transfer at the transition state. Because of other possible contributions such as the “baseline” k_0 value and the push–pull effect, this interpretation can only be tentative.

Experimental Section

Materials. The pentacarbonyl(cyclobutenylidene)chromium complexes **1d** and **1e** were available from a previous study.¹ **3b** was synthesized as described in the literature.²⁹ The product was dried and purified by column chromatography with 90:10 hexane ether. The solution volume was reduced, crystals were collected at 0°C and dried under vacuum. ¹H NMR δ (CDCl₃): 1.23 (6H, d, (CH₃)₂), 3.45 (1H, m, H), 3.95 (6H, 2s, N(CH₃)₂).

P2-Et was purchased from Fluka. Acetonitrile was dried over P₂O₅ and distilled under nitrogen.

pK_a Measurements. A detailed description of the methodology has been reported before,⁶ and hence, only a brief summary is presented here. The pK_a of the carbene complexes (pK_a^{CH}) is given by eq 7 where BH⁺ refers to the protonated form of **P2-Et** and K₁, the equilibrium constant for the ionization equilibrium CH + B \rightleftharpoons C⁻ + BH⁺, is defined by eq 8.

$$pK_a^{CH} = pK_a^{BH^+} - \log K_1 \quad (7)$$

$$K_1 = \frac{[C^-] + [BH^+]}{[CH][B]} \quad (8)$$

The concentration of the free carbene complex ([CH]) is related to its total concentration ([CH]₀) by eq 9 where r is given by eq 10 and A refers to the absorbance at intermediate **P2-Et**

$$[CH] = r[CH]_0 \quad (9)$$

$$r = \frac{A - A_\infty}{A_0 - A_\infty} \quad (10)$$

concentrations (partial conversion of CH to its anion C⁻), A₀ to the absorbance in the absence of **P2-Et** (no conversion of CH to C⁻), and A_∞ to the absorbance of high [**P2-Et**] (complete conversion of CH to C⁻). The concentration of the other species

are calculated as shown in eqs 11 and 12.

$$[C^-] = [BH^+] = (1 - r)[CH]_0 \quad (11)$$

$$[B] = [B]_0 - [BH^+] \quad (12)$$

K₁ values for a given carbene complex were determined for 11–16 different sets of [CH]₀ and [B]₀; the raw data are summarized in Tables S5–S7 of the Supporting Information.⁹ The pK_a^{CH} values reported in Table 1 represent the averages of these determinations.

Computational Studies. All computations were carried out using the GAUSSIAN 98 suite of programs.³⁰ Calculations were performed at the HF and B3LYP levels of theory using a generalized basis set. The Way–Hadt effective core potential³¹ was assigned to the chromium atom, the 6-31+G* basis set was used for the atoms that are part of the reacting system (**1d**, **1d**⁻, **1e**, and $1e^-$: four-membered ring atoms, N; **3a** and **3b**: C of CHR₂, N; **5** and 5^- : five-membered ring atoms, N), while the 3-21G* basis set was assigned to the atoms that are not part of the reacting system (**1d** and **1e**: Me, R', Et₂, H, (CO)₅; **1d**⁻ and $1e^-$: Me, R', Et₂, (CO)₅; **3a** and **3b**: Me₂, (CO)₅, H; **3a**⁻ and **3b**⁻: Me₂, (CO)₅; **5** and 5^- : Me, Et₂, (CO)₅). The geometries of all neutral carbene complexes and their respective anions were first optimized at the HF level and then further optimized at the B3LYP level. For $1e^-$, the initial geometry was constrained in such a way that the length of the C1–C2 bond corresponded to that of the B3LYP C1–C3 bond in $1e^-$, the C1–C3 bond to that of the B3LYP C1–C2 bond in $1e^-$, and the C2–C4 to that of the B3LYP C3–C4 bond in $1e^-$. The structure of $1e^{*-}$ constrained in this manner was then optimized at the B3LYP level.

Frequency calculations were performed at the B3LYP level and contributions to the vibrational partition functions were scaled with the scaling factor 0.9613 according to Scott and Radom.³² The acidities were calculated as

$$\Delta H^{\circ} = \Delta E + \Delta ZPE + \Delta C_{\text{vib}}RT \quad (13)$$

where ΔE is the difference in electronic energy at a given level of theory, ΔZPE the difference in the scaled zero-point energies and $\Delta C_{\text{vib}}RT$ the difference in the scaled vibrational heat capacities.

Acknowledgment. This research has been supported by Grant No. CHE-0098553 from the National Science Foundation. Partial support of V.R. by the Department of Education in the form of a GAANN fellowship is also gratefully acknowledged.

Supporting Information Available: Tables S1–S3 (geometries), S4 (energies), and S5–S7 (pK_a determinations) and structures S1–S10 (Z-matrices). This material is available free of charge via the Internet at <http://pubs.acs.org>.

JO040168T

(30) Frisch, M. J.; Trucks, G. W.; Schlegel, H. B.; Scuseria, G. E.; Robb, M. A.; Cheeseman, J. R.; Zakrzewski, V. G.; Montgomery, J. A., Jr.; Stratmann, R. E., Jr.; Burant, J. C.; Dapprich, S.; Millam, J. M.; Daniels, A. D.; Kudin, K. N.; Strain, M. C.; Farkas, O.; Tomasi, J.; Barone, V.; Cossi, M.; Cammi, R.; Mennucci, B.; Pomelli, C.; Adamo, C.; Clifford, S.; Ochterski, J.; Petersson, G. A.; Ayala, P. Y.; Cui, Q.; Morokuma, K.; Malick, D. K.; Rabuck, A. D.; Raghavachari, K.; Foresman, J. B.; Cioslowski, J.; Ortiz, J. V.; Stefanov, B. B.; Liu, G.; Liashenko, A.; Piskorz, P.; Komaromi, I.; Gomperts, R.; Martin, R. L.; Fox, D. J.; Keith, T.; Al-Laham, M. A.; Peng, C. Y.; Nanayakkara, A.; Gonzalez, C.; Challacombe, M.; Gill, P. M. W.; Johnson, B.; Chen, W.; Wong, M. W.; Andres, J. L.; Gonzalez, C.; Head-Gordon, M.; Replogle, E. S.; Pople, J. A. *GAUSSIAN 98*, Revision a.7; Gaussian, Inc., Pittsburgh, PA, 1998.

(31) (a) Hay, P. J.; Wadt, W. R. *J. Chem. Phys.* **1985**, *82*, 270. (b) Hay, P. J.; Wadt, W. R. *J. Chem. Phys.* **1985**, *82*, 270.

(32) Scott, A.; Radom, L. *J. Phys. Chem.* **1996**, *100*, 16502.

(29) (a) Aumann, R.; Fischer, E. O. *Angew. Chem., Int. Ed. Engl.* **1967**, *6*, 879. (b) Connor, J. A.; Fischer, E. O. *J. Chem. Soc. A* **1969**, 578.